Muscle-derived Dpp regulates feeding initiation via endocrine modulation of brain dopamine biosynthesis
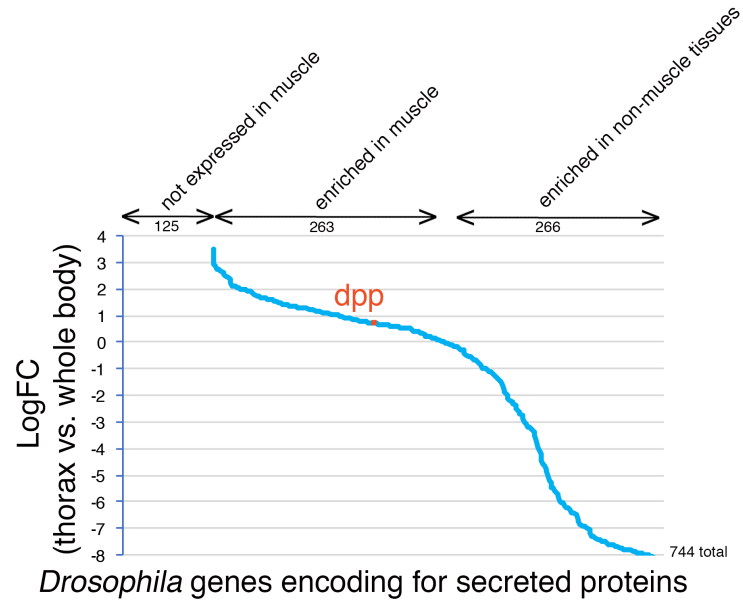
Maricela Robles-Murguia, Deepti Rao, David Finkelstein, Beisi Xu, Yiping Fan, Fabio Demontis

Supplemental Figures S1–S9

Supplemental Table S1

Supplemental References

Drosophila genes encoding for secreted proteins

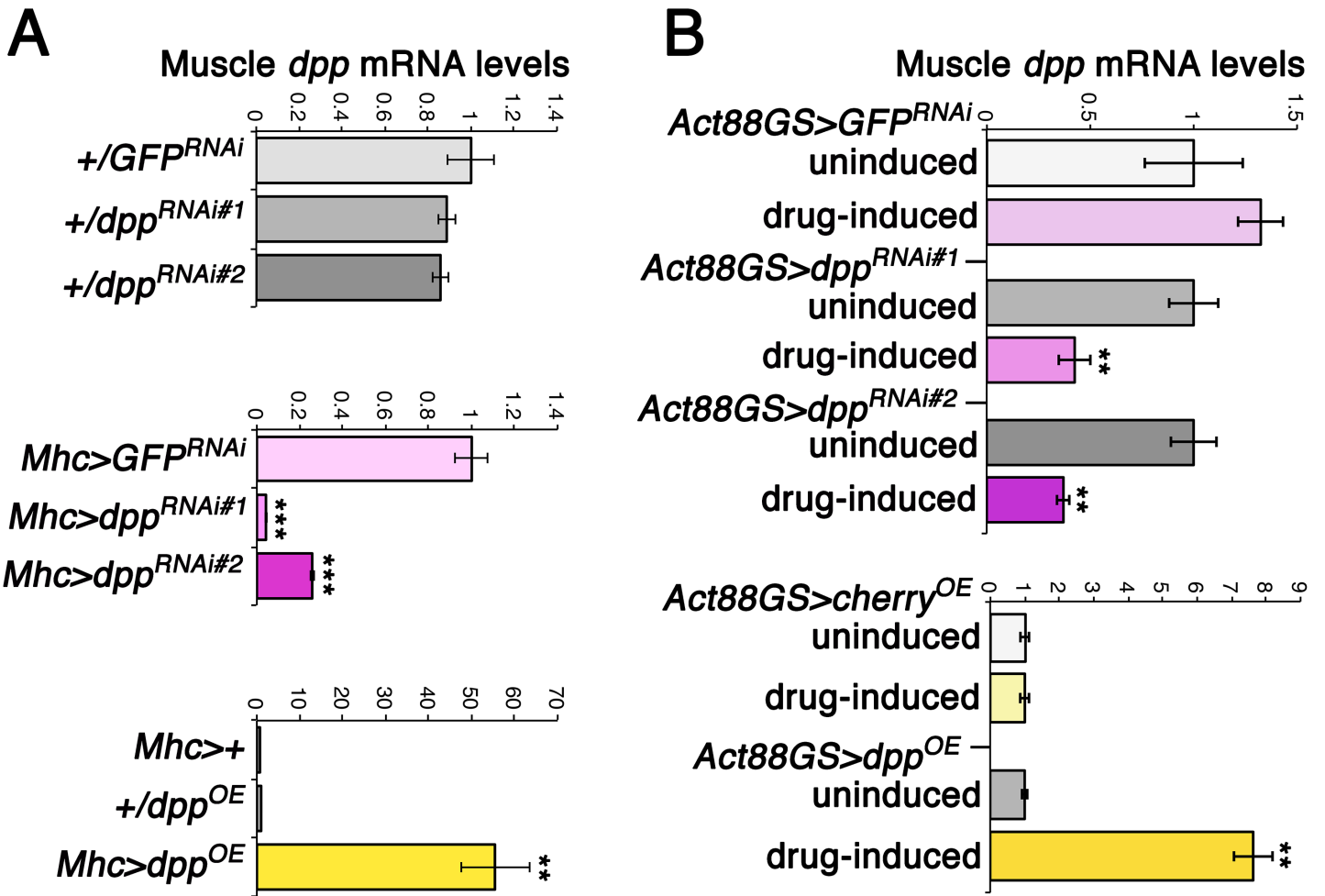|	logFC	PValue
dpp	0.67311221	8.40778E-07

Supplemental Figure S1. *dpp* **is expressed in skeletal muscle of adult** *Drosophila*.
RNA-seq analyses of transcriptomes from *Drosophila* thoraces, which consist primarily of skeletal muscle, and the whole body. The *y* axis reports the logFC of gene expression changes in thoraces versus the whole body whereas the *x* axis corresponds to the 744 genes that are predicted to encode for secreted proteins in *Drosophila*. Of these, 125 are not expressed in muscle, 263 have enriched expression in muscle compared to the whole body (LogFC>0.5, *p*<0.05), and 266 are enriched in non-muscle tissues (LogFC<-0.5, *p*<0.05). *dpp* has enriched expression in skeletal muscle versus the whole body.
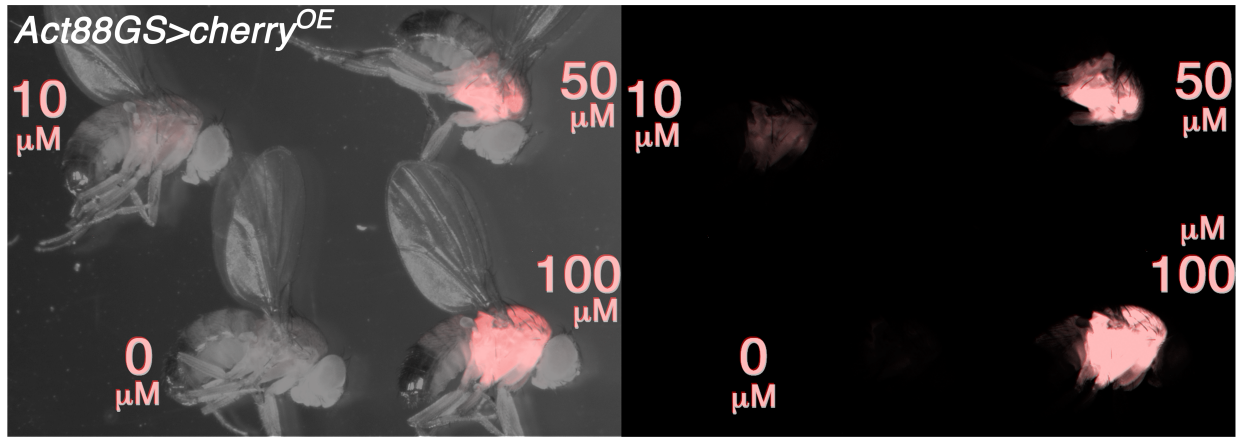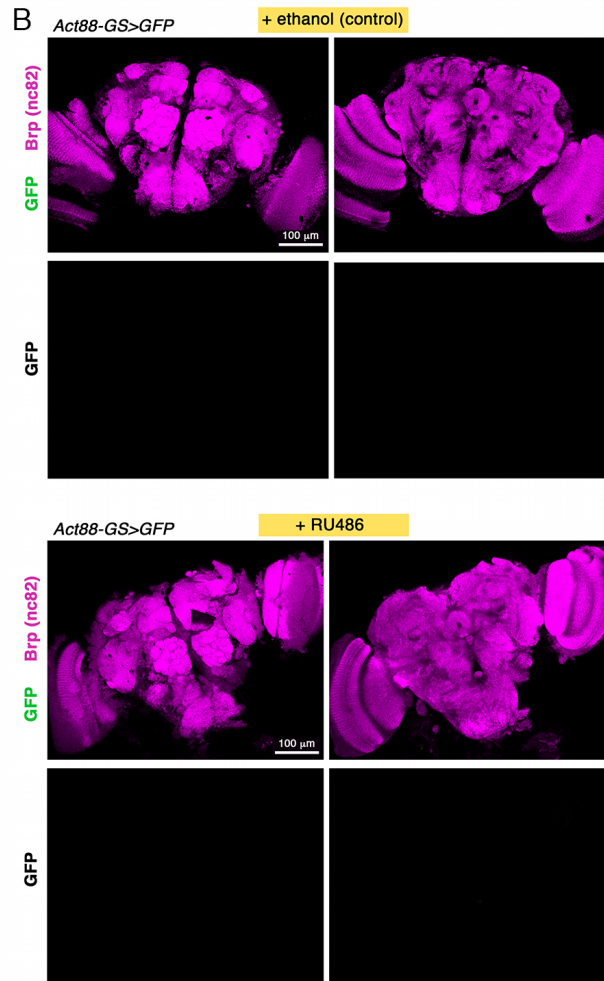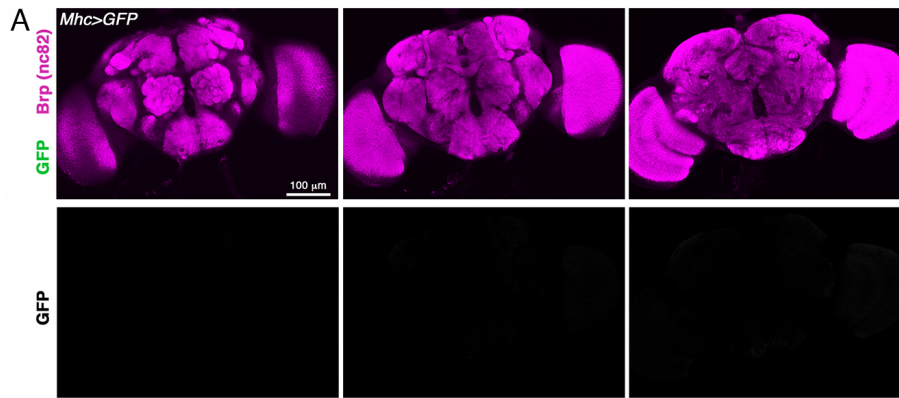
Supplemental Figure S2. Characterization of the drug-inducible, skeletal muscle-specific *Act88-GeneSwitch-Gal4* driver.

Act88-GS-Gal4 (Robles-Murguia et al. 2019) drives transgenic expression in the presence of RU486 in the food, as shown by fluorescence in *Act88GS>cherry*[OE] flies fed food having a final concentration of 10, 50, or 100 μM RU486, compared with control flies (ethanol control; 0 μM RU486). In these flies, a 2-kb *Act88F* promoter region drives *GS-Gal4* expression. As expected, according to the exclusive expression of *Act88F* in skeletal muscle (primarily indirect flight muscles, (Nongthomba et al. 2001)), no apparent *cherry* transgene expression is detected outside of the fly thorax, where indirect flight muscles are located, indicating that *Act88-GS-Gal4* is specific to skeletal muscle.

A

Muscle *dpp* mRNA levels

(bar chart with categories: +/GFP^RNAi, +/dpp^RNAi#1, +/dpp^RNAi#2; x-axis 0 to 1.4)

(bar chart with categories: Mhc>GFP^RNAi, Mhc>dpp^RNAi#1 ***, Mhc>dpp^RNAi#2 ***; x-axis 0 to 1.4)

(bar chart with categories: Mhc>+, +/dpp^OE, Mhc>dpp^OE **; x-axis 0 to 70)

B

Muscle *dpp* mRNA levels

(bar chart with categories: Act88GS>GFP^RNAi uninduced, drug-induced; Act88GS>dpp^RNAi#1 uninduced, drug-induced **; Act88GS>dpp^RNAi#2 uninduced, drug-induced **; x-axis 0 to 1.5)

(bar chart with categories: Act88GS>cherry^OE uninduced, drug-induced; Act88GS>dpp^OE uninduced, drug-induced **; x-axis 0 to 9)

Supplemental Figure S3. Modulation of dpp mRNA levels in response to dpp RNAi and overexpression in skeletal muscle. (*A–B*) qRT–PCR analyses of skeletal muscle in which *dpp* mRNA levels are modulated via the Gal4/UAS system (Brand and Perrimon 1993) and the skeletal muscle–specific drivers *Mhc-Gal4* and *Act88-GS-Gal4*. (*A*) As expected, dpp RNAi driven by *Mhc-Gal4* reduces dpp mRNA levels whereas *dpp* overexpression increases them, compared with controls. (*B*) Similar results are obtained with the drug-inducible *Act88-GS-Gal4* driver, compared with uninduced controls. In (*A–B*), SEM is shown with n=4, **p<0.01, ***p<0.001.

4

Supplemental Figure S4. The skeletal muscle-specific *Mhc-Gal4* and *Act88-GeneSwitch-Gal4* drivers do not drive transgene expression in the brain.

(*A–B*) Brains from flies with cytosolic GFP transgenic expression driven by (*A*) *Mhc-Gal4* and (*B*) *Act88-GeneSwitch-Gal4*. No GFP fluorescence is detected in the brains of *Mhc>GFP* and (*B*) *Act88-GS>GFP* flies, as expected based on the characterization of these drivers as skeletal muscle-specific (Schuster et al. 1996; Demontis and Perrimon 2010; Robles-Murguia et al. 2019). The overall brain architecture is shown with immunostaining with anti-Brp antibodies (pink). The scale bar is 100 µm.
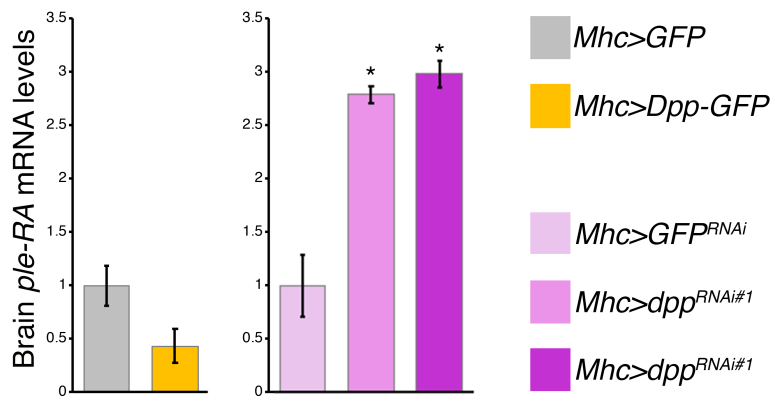
Supplemental Figure S5. Modulation of *dpp* in skeletal muscle regulates brain expression of *ple-RA*, a brain-specific isoform of *pale*. qRT-PCR analyses of brains from flies in which *dpp* mRNA levels are modulated via the Gal4/UAS system and the skeletal muscle-specific driver *Mhc-Gal4*. As expected based on Fig. 2C-D, muscle-specific dpp RNAi increases brain *ple-RA* expression whereas muscle-specific *dpp* overexpression reduces it, compared with controls. SEM is shown with n=4, *$p<0.05$.
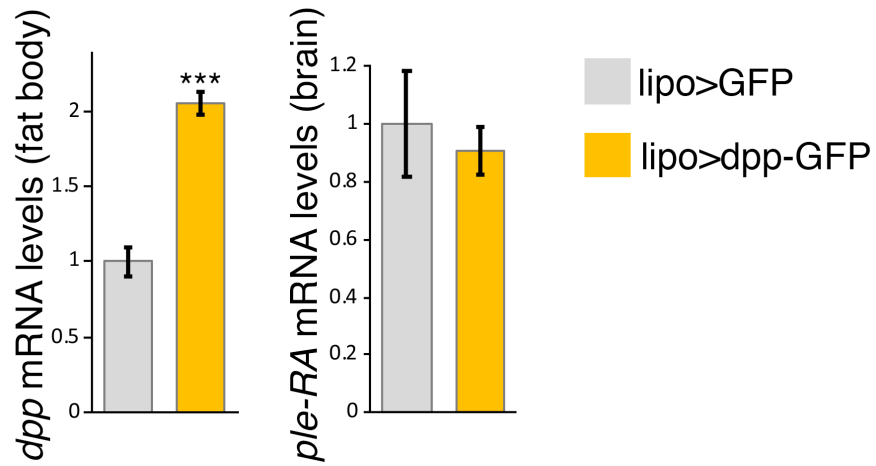
Supplemental Figure S6. Fat body-specific overexpression of *dpp* with *lipophorin-Gal4*.
Similar to muscle-derived Dpp, Dpp released by non-muscle tissues may also contribute to regulate brain *TH/ple*. However, only a minimal decrease in *TH/ple* expression is seen in response to *dpp* overexpression in the fat body in presence of *tubulin-Gal80ts* at 29°C. Specifically, a 2-fold increase in abdominal *dpp* levels leads to a ~10% decrease in the expression of *ple-RA*, a brain-specific isoform of *pale*. SEM is shown with n=4, ***p<0.001.
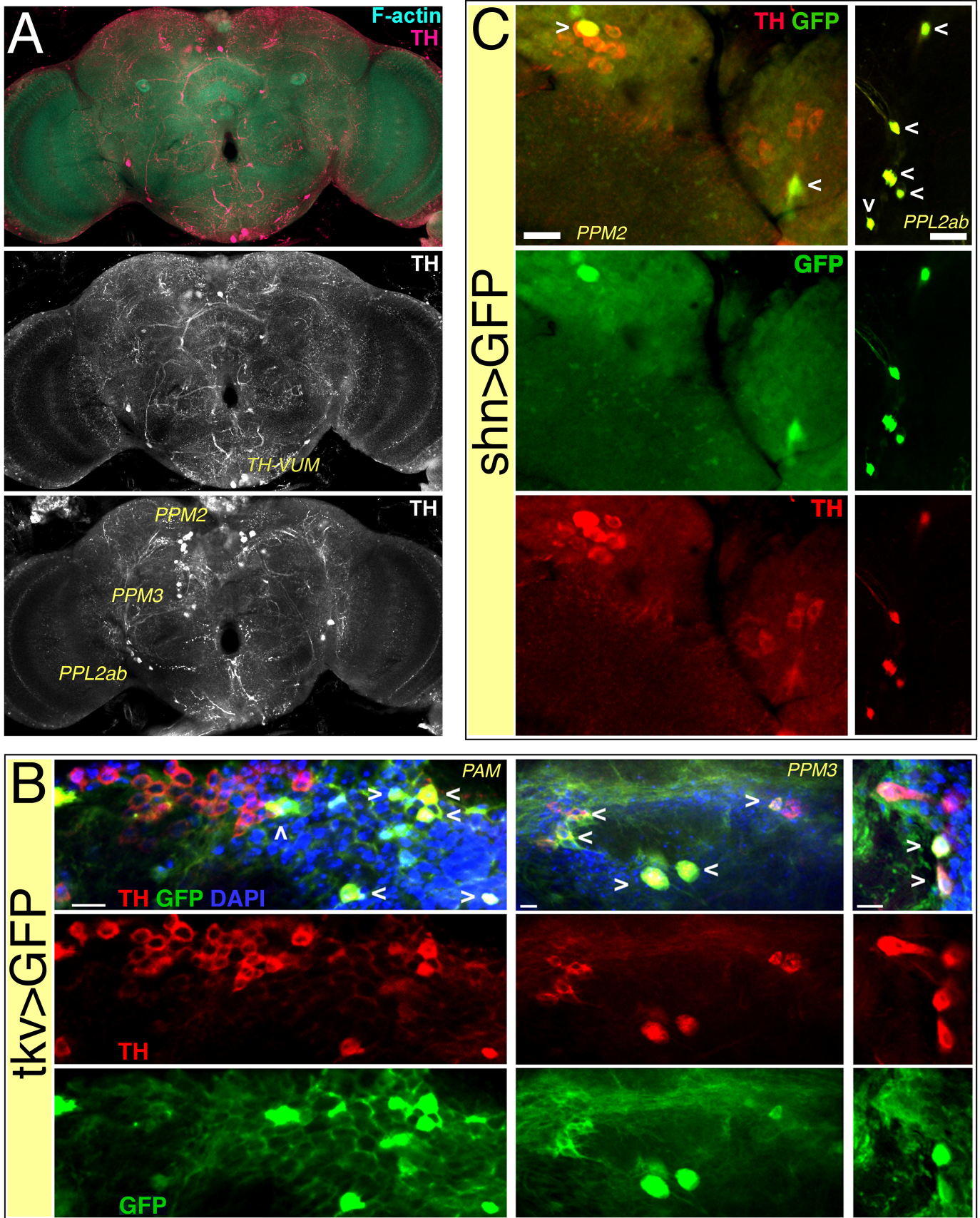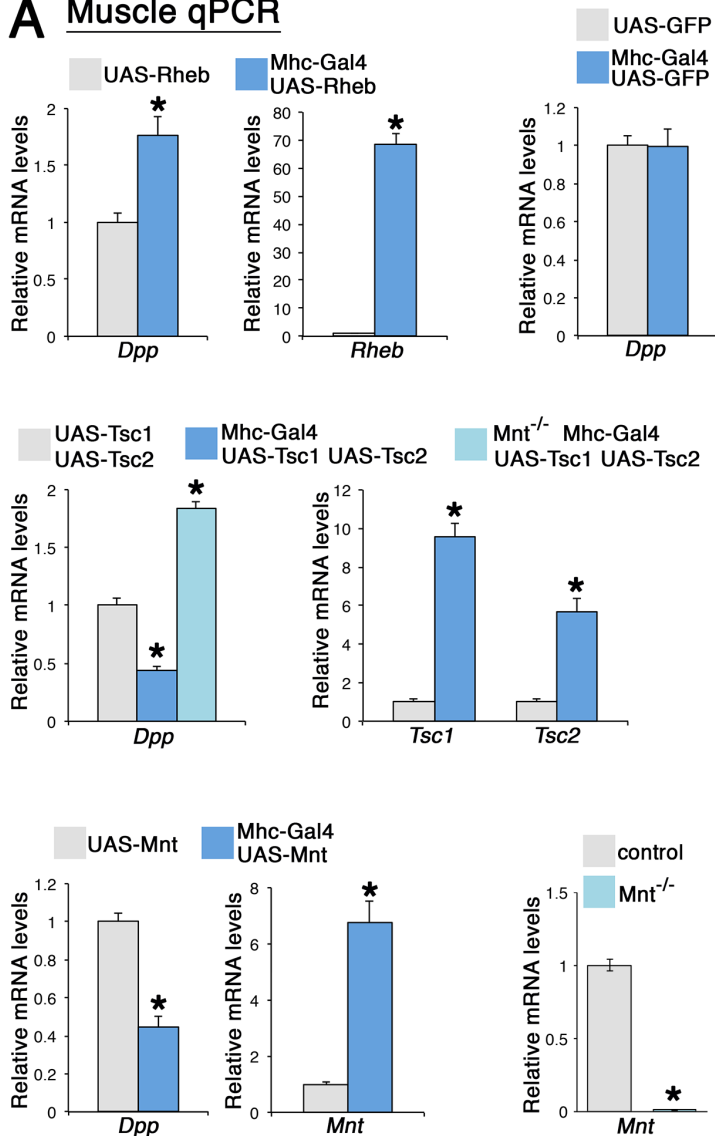
Supplementary Figure S7

Supplemental Figure S7. Dopaminergic neurons express Dpp receptor signal transduction components. (*A*) Immunostaining of brains with anti-TH antibodies identifies previously described clusters of dopaminergic neurons (Mao and Davis 2009), including the TH-VUM previously implicated in the PER (Marella et al. 2012). Alexa635-phalloidin staining is used to detect F-actin and highlight overall brain architecture. Names of some dopaminergic neuronal clusters, based on (Mao and Davis 2009), are indicated in yellow in (*A-C*). (*B*) Immunostaining of brains from *tkv>GFP* flies with anti-TH antibodies indicates that some TH-positive dopaminergic neurons display high *GFP* expression and therefore potentially have high expression of the Dpp receptor *tkv*. (*C*) Similarly, brains from *shn>GFP* flies have TH-positive dopaminergic neurons that display high *GFP* expression, which may indicate a high expression of the transcriptional repressor *shn*.
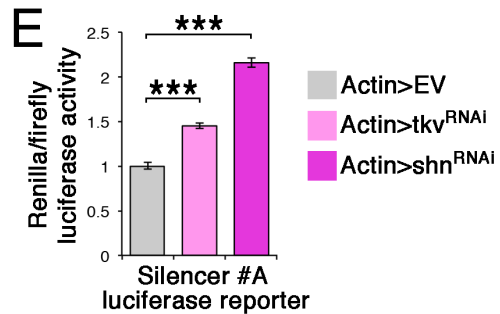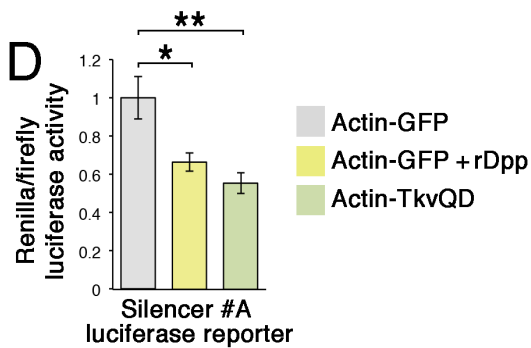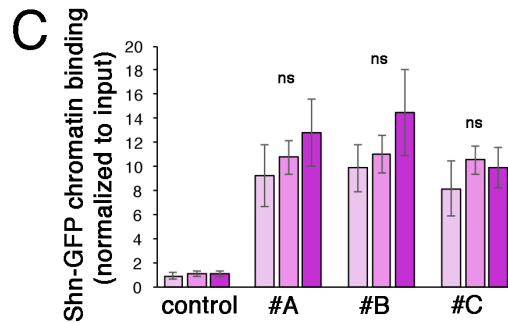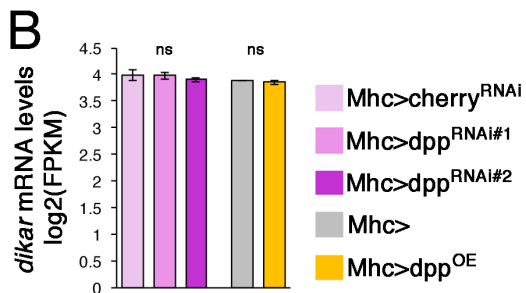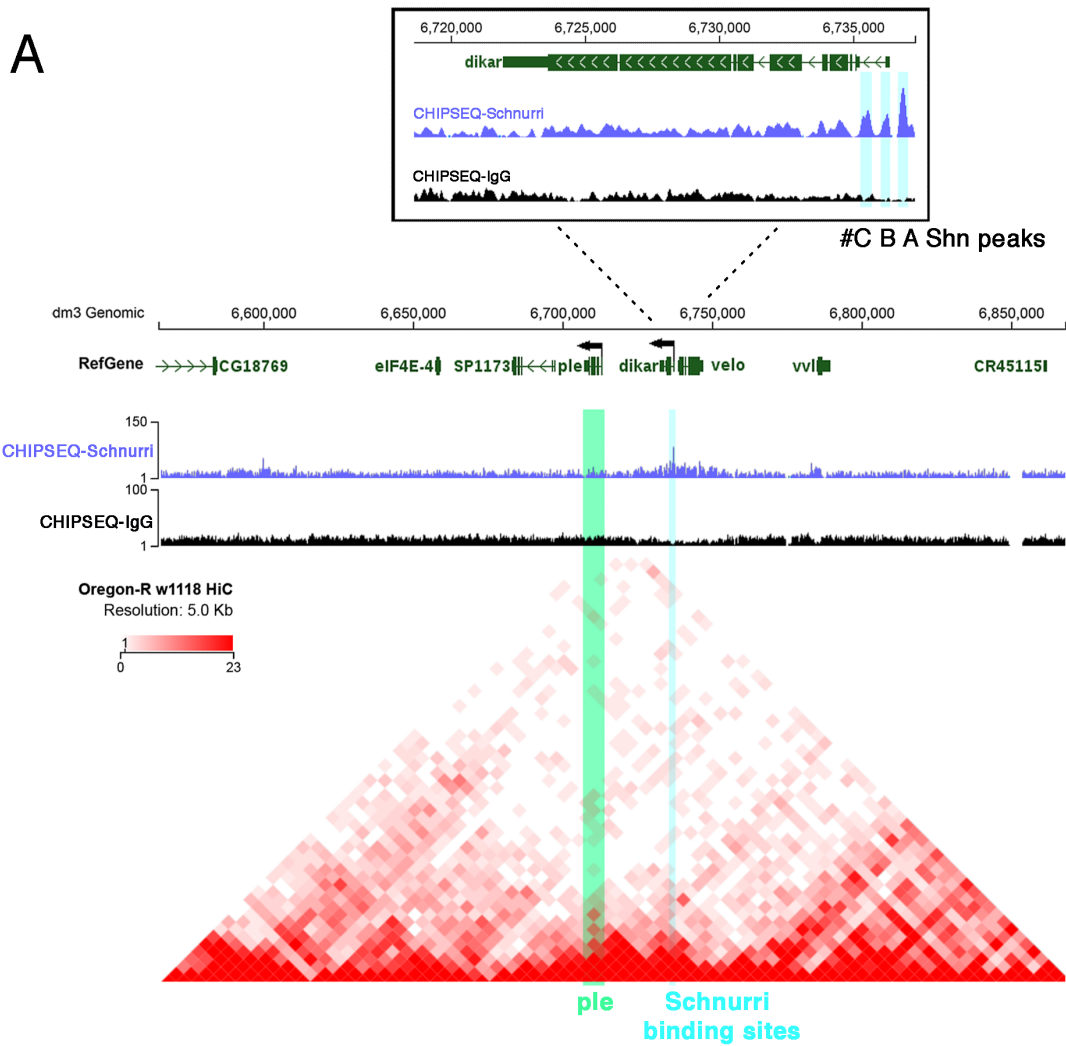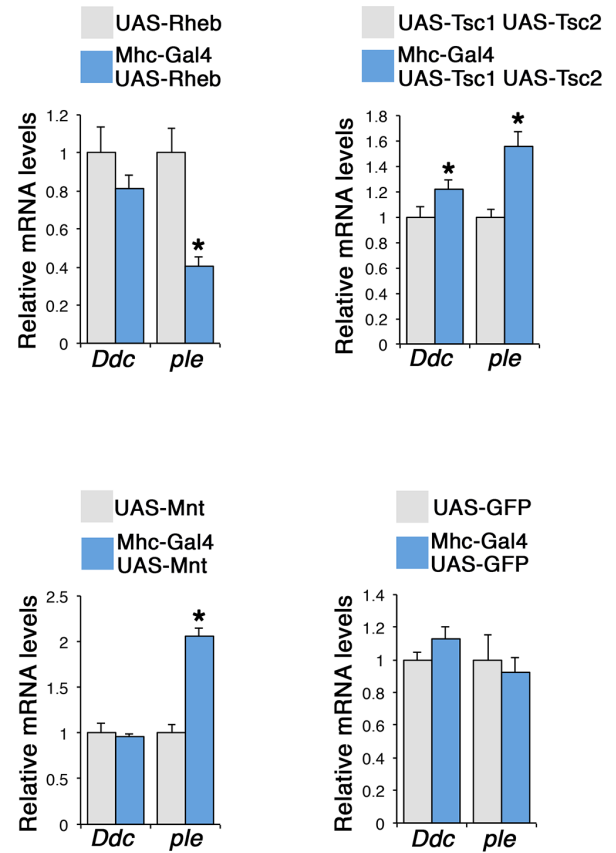
Supplementary Figure S8

Supplemental Figure S8. A region located near *dikar* is bound by Shn and modulates *ple/TH* expression in response to Dpp. (*A*) ChIP-seq data analysis indicates that Shn binds to a region proximal to *dikar*, a gene located near *ple*. Analysis of Hi-C data indicates that this region with Shn binding is located in the same topologically associated domain (TAD) as the *ple* promoter. (*B*) Gene expression profiling indicates that Dpp does not modulate *dikar* expression, suggesting that the *dikar* promoter region characterized by ChIP-seq Shn peaks may work as a silencer for *ple* expression; log(2)FPKM values are shown, with n=3 and SEM (ns= not significant). (*C*) Consistent with a previous study reporting that Mad, Medea, and Schnurri are bound to DNA also in the absence of Dpp signaling (Van Bortle et al. 2015), ChIP-qPCR experiments indicate that Shn-GFP binding to the *dikar* promoter does not change in response to muscle-restricted *dpp* RNAi, suggesting that Dpp signaling modulates Shn activity in its DNA-bound state; n=3, SD. Genotype information for (*B-C*) is provided in (*B*). (*D-E*) Luciferase assays in *Drosophila* S2R+ cells with a *Renilla* luciferase reporter based on the *dikar* region bound by Shn (ChIP-seq peak #A). (*D*) Promotion of Dpp signaling after administration of recombinant Dpp (rDpp; n=14) or expression of a constitutively active version of the Dpp receptor Tkv (Tkv^{QD}; n=7) reduces luciferase activity, compared with control *GFP* expression (n=14). These findings suggest that Dpp signaling decreases *ple/TH* expression via a silencer region in the proximity of *dikar* which is bound by Shn and is in the same TAD of the *ple/TH* promoter. (*E*) Consistently, RNAi for the Dpp receptor Tkv and for the transcriptional repressor Shn leads to higher luciferase activity (n=15). In (*D-E*), SEM is indicated with *p<0.05, **p<0.01, ***p<0.001; ns, not significant.

Supplemental Figure S9. The target of rapamycin (mTOR) nutrient-sensing pathway regulates *dpp* **gene expression in skeletal muscle via the transcription factor Mnt.** (*A*) qRT-PCR from skeletal muscle with activation of mTOR signaling (obtained via *Rheb* overexpression) and inhibition (obtained via overexpression of the tuberous sclerosis complex, formed by Tsc1 and Tsc2). *Rheb* overexpression increases *dpp* mRNA levels, compared to *GFP* and transgene alone controls. Conversely, overexpression of the tuberous sclerosis complex *Tsc1+Tsc2* (an inhibitor of mTOR) reduces *dpp* gene expression via the transcription factor Mnt. Specifically, *Mnt* overexpression similarly inhibits *dpp* gene expression whereas *Tsc1+Tsc2* overexpression reduces *dpp* mRNA levels in wild-type but not in *Mnt* null muscle. (*B*) qRT-PCR from brains indicates that *TH/ple* expression is modulated in a manner consistent with the modulation of muscle *dpp* levels, whereas *Ddc* expression is typically not regulated. In (*A-B*), SEM is indicated with n=3 and *$p<0.05$.

Supplemental Table S1. RNA-sequencing data from heads of flies with skeletal muscle-specific *dpp* overexpression and dpp RNAi. The fold changes (logFC) versus the control samples are indicated, as well as the significance score, which corresponds to -log10(*p*-value). Two different dpp RNAi (#1 and #2) were used.

SUPPLEMENTAL REFERENCES

Brand AH, Perrimon N. 1993. Targeted gene expression as a means of altering cell fates and generating dominant phenotypes. *Development* **118**: 401-415.

Demontis F, Perrimon N. 2010. FOXO/4E-BP signaling in Drosophila muscles regulates organism-wide proteostasis during aging. *Cell* **143**: 813-825.

Mao Z, Davis RL. 2009. Eight different types of dopaminergic neurons innervate the Drosophila mushroom body neuropil: anatomical and physiological heterogeneity. *Front Neural Circuits* **3**: 5.

Marella S, Mann K, Scott K. 2012. Dopaminergic modulation of sucrose acceptance behavior in Drosophila. *Neuron* **73**: 941-950.

Nongthomba U, Pasalodos-Sanchez S, Clark S, Clayton JD, Sparrow JC. 2001. Expression and function of the Drosophila ACT88F actin isoform is not restricted to the indirect flight muscles. *J Muscle Res Cell Motil* **22**: 111-119.

Robles-Murguia M, Hunt LC, Finkelstein D, Fan Y, Demontis F. 2019. Tissue-specific alteration of gene expression and function by RU486 and the GeneSwitch system. *npj Aging and Mechanisms of Diseasevolume* **5**.

Schuster CM, Davis GW, Fetter RD, Goodman CS. 1996. Genetic dissection of structural and functional components of synaptic plasticity. I. Fasciclin II controls synaptic stabilization and growth. *Neuron* **17**: 641-654.

Van Bortle K, Peterson AJ, Takenaka N, O'Connor MB, Corces VG. 2015. CTCF-dependent co-localization of canonical Smad signaling factors at architectural protein binding sites in D. melanogaster. *Cell Cycle* **14**: 2677-2687.